Progress In Electromagnetics Research, Vol. 139, 289–301, 2013

A NOVEL POWER DIVIDER INTEGRATED WITH SIW AND DGS TECHNOLOGY

Zhaosheng He, Jingye Cai, Zhenhai Shao*, Xiang Li, and Yongmao Huang

School of Communication and Information Engineering, University of Electronics Science and Technology of China, Chengdu 611731, China

Abstract—In this paper, a novel power divider integrated with substrate integrated waveguide (SIW) and defected ground structures (DGS) techniques is proposed to provide both power dividing and filtering functions. The SIW technique holds advantages of low profile, low-lost, mass-production, easy fabrication and fully integration with planar circuits. By integrating with defected ground structures (DGS) technique, the size and cost of system can be effectively reduced as the proposed power divider has a function of filtering which leads to reduction of one filter. In order to verify the design approach, the proposed power divider with equal power divisions at the center frequency of 8.625 GHz is fabricated and measured. The measured results demonstrate that the insertion loss is less than 1.2 dB and the input return loss less than 16 dB across the bandwidth of 1.4 GHz (FBW is 16%). Moreover, the imbalances of the amplitude and phase are less than 0.3 dB and 0.5 degree, respectively.

1. INTRODUCTION

As a fundamental unit of microwave and millimeter-wave circuits, power divider is a kind of microwave network that can split signal into different routines with equal or unequal power division ratio. It is largely utilized in the satellite communications, electronic warfare systems, testing systems and phased array radars. Its insertion loss, output port matching and amplitude/phase imbalances are key specifications when it is used to build microwave and millimeter-wave circuits and subsystems.

In the early days, power splitting techniques have focused on waveguide-based power dividing techniques due to their high power

Received 20 February 2013, Accepted 8 April 2013, Scheduled 29 April 2013

* Corresponding author: Zhenhai Shao (shao_zh@uestc.edu.cn).

handling capacity, low-loss and good heat sink. However, those components are generally massive and require high precision machining processes which lead to heavy difficulties for mass production. Besides, they are not easy to be integrated with planar structure circuits because of their three-dimensional structure.

For low power applications, power dividers are implemented based on microstrip line because of small size and light weight. The Wilkinson power divider has been widely used with advantages that its output ports can be simultaneously isolated and matched, as well as its bandwidth is extremely wide [1]. Although a large number of designs focusing on minimizing size [2–8] or obtaining unequal power division ratio [9–14] have been reported, some of them have poor power handling capability and tend to have high radiation loss, which make them to be poor choices for microwave and millimeter-wave circuit applications.

Recently a new planar structure which called substrate integrated waveguide (SIW) was proposed [15, 16]. SIW is a kind of integrated waveguide structure which is implemented by metallic vias on low loss dielectric substrate through PCB fabrication process [17, 18]. Compared with traditional waveguide structures, it is low loss, mass productive and easily integrated with planar circuits so that it provides a useful technology to design microwave and millimeter-wave components with high performance and low cost, such as filters, couplers, diplexers, power dividers and antennas. Similar to conventional rectangular waveguide, TE_{m0}-like modes can be propagated in a SIW. Here, the field distribution of the dominant TE_{10}-like mode is shown in Figure 1.

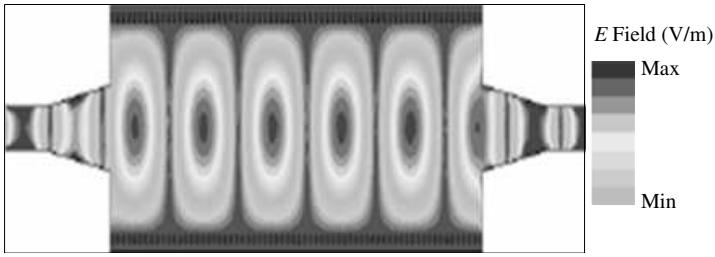

Figure 1. Field distribution of the dominant TE_{10}-like mode in SIW.

The band pass filter (BPF) is another important passive component which is indispensable device in RF systems as it is used to separate the desirable frequency and reject unwanted signals in a complex electronic-magnetic environment. In order to split and select useful signals, many microwave systems contain the power divider and

filter at the same time, which leads to large size, high insert ion loss of the system.

Therefore, it is demanded to integrate the two components into one device to realize power dividing and filtering functions. In this paper, a novel low loss, band-pass power divider which is based on substrate integrated waveguide (SIW) and defected ground structure (DGS) techniques is proposed. When the proposed device is applied in microwave and millimeter-wave systems, the size, loss and cost of the systems can be effectively reduced. Details of the proposed band pass power divider are presented in the following parts.

2. DESIGN OF THE POWER DIVIDER

2.1. SIW Power Divider with T-junction Configuration

The structure of a typical SIW power divider is shown in Figure 2. It is consisted of two perpendicular SIW structures, three SIW to microstrip line transitions and an inductive post. In Figure 2, W_{taper} and l_{taper} are the width and the length of transition, respectively. D_{post} is the

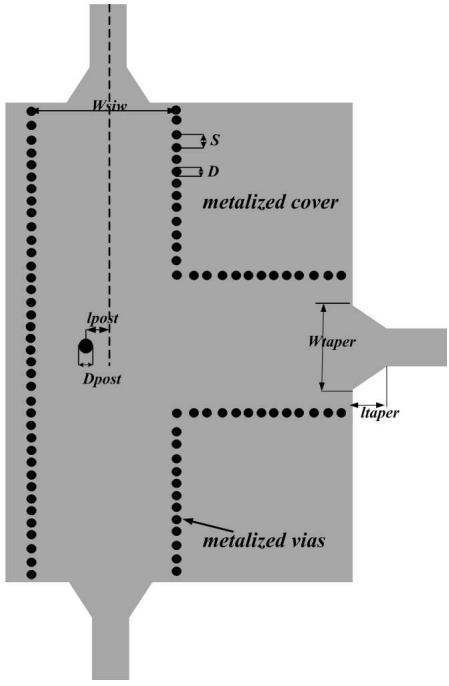

Figure 2. SIW power divider with T-junction configuration.

diameter of inductive post, as well as l_{post} is the distance between the center of the post and the center of SIW.

For convenient connection of the power divider to other components and for testing convenience, three tapered lines are used to act as transitions from the SIW to 50 Ω microstrip line. Another function of the tapered lines is to match the impedance between the SIW and 50 Ω microstrip line. The 50 Ω microstrip line with quasi-TEM mode can excite a TE_{10} mode well and both microstrip line and SIW have approximated electric field distributions in the profile of the structure.

The inductive post which is short circuited between the up and down sides of SIW is placed at the center of the power divider. According to basic waveguide transmission theory, the inductive post is equivalent to a parallel susceptance. It can suppress reflection in a wide frequency band. By changing the diameter and position of the inductive post, the reflecting and scattering signal of the input signals can be easily adjusted. Another function of the cylindrical post is to match the output port as the three ports of metallic waveguide T junction power divider cannot be matched simultaneously [19]. The cut-off frequency of the SIW power divider is designed at 8.0 GHz and the initial dimensions can be calculated by empirical formula (1) and formula (2) with good precision under conditions of $S/D < 3$ and $W_{\text{siw}}/D > 10$ [20, 21].

$$W = W_{\text{siw}} - 1.08\frac{D^2}{S} + 0.1\frac{D^2}{W_{\text{siw}}}, \tag{1}$$

$$f_c = \frac{1}{2W\sqrt{\varepsilon_r}}, \tag{2}$$

where f_c is the cut-off frequency of metallic rectangular waveguide, and ε_r is the relative permittivity of the substrate. W represents the width of the corresponding metallic rectangular waveguide, W_{siw} is the width of SIW waveguide, D is the diameter of metallic via holes, and S is the distance between two vias.

The cut-off frequency is almost monotonously determined by the width of SIW structure from formula (1). Therefore, what needed to be optimized to realize the output port matching after the modelling of SIW structures are the dimensions of SIW-microstrip line transitions, and the size as well as location of the inductive post. According to the recommendation of [19], the diameter of the post, D_{post}, is optimized to reduce the reflection with initial value of 1/4 waveguide wavelength. The location of the post, l_{post}, is optimized to get minimum value of reflection. The optimization procedure is finished by electromagnetic (EM) simulation tools.

2.2. Design and Analysis of the Proposed DGS Cell

Defected ground structures (DGS) was first proposed by Korean scholar J. I. Park in 1999 based on studying of PBG structure, and then it became a research hotspot [22]. DGS is implemented by etching periodic or non-periodic cascaded configuration defect in the ground of transmission lines such as microstrip and coplanar lines. The shield current distribution in the ground plane is disturbed because of the etched DGS, which will change the characteristics of a transmission line such as equivalent capacitance and inductance [23]. The DGS technique usually utilizes an artificial defect in the ground to provide a band-rejection characteristic [24]. Many different types of DGS cells have been used in filter design to improve the stop band characteristics with band-rejection properties [25].

Figure 3(a) shows a schematic of the proposed DGS unit cell. The difference from traditional DGS is that the proposed DGS is etched in the top plane of SIW which brings consistency of ground plane when it is applied in the system. When excited by outside port, it behaves as a parallel resonant unit which leads to bandstop characteristics. It can be modeled by LC circuit as shown in Figure 3(b) [24]. The parameters in the equivalent circuit can be determined using the following equations [25]:

$$C_p = \frac{5f_c}{\pi\left[f_p^2 - f_c^2\right]} \text{ pF}, \tag{3}$$

$$L_p = \frac{25}{C_p\left(\pi f_p\right)^2} \text{ nH}, \tag{4}$$

where f_c and f_p are the 3-dB edge frequency and the attenuation pole frequency in GHz, respectively. The dimensions of the DGS unit cell determine the resonant frequency of the cell [26]. Figure 4 shows the

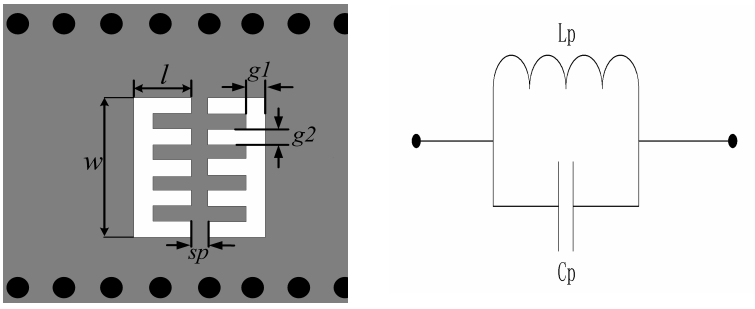

Figure 3. (a) Schematic of DGS cell. (b) Equivalent circuit.

simulated result of this cell. From the results, it can be seen that the designed unit DGS provides a band-rejection property of 45 dB suppression at 12 GHz. And compared with traditional dumbbell DGS, the proposed DGS structure provides deeper attenuation and sharper cut-off edge.

In order to investigate the bandstop characteristic, the proposed DGS with different dimensions are studied. Figure 5 shows the variation of S_{21} parameter against the variation of the length l and the width w, and Figure 6 for $g1$ and $g2$ respectively.

From Figure 5, it can be seen that with the increment of w or l, the upper bandgap point moves to lower frequency. And an identical phenomenon appears with increase of $g2$ or decrease of $g1$ as shown in Figure 6. In both of Figures 5 and 6, the lower frequency almost keeps the same as it is the cutoff frequency of SIW which is monotonously

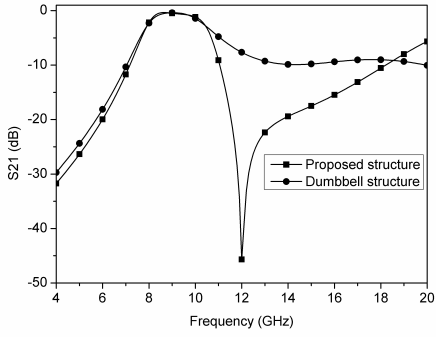

Figure 4. Simulated results of proposed and traditional dumbbell DGS.

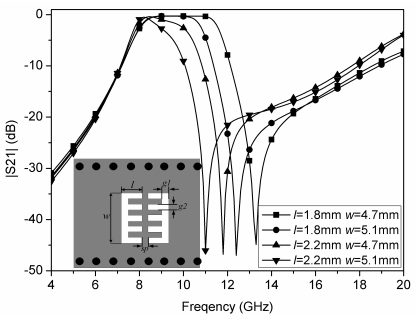

Figure 5. Simulated results of proposed DGS cell with variation of l and w.

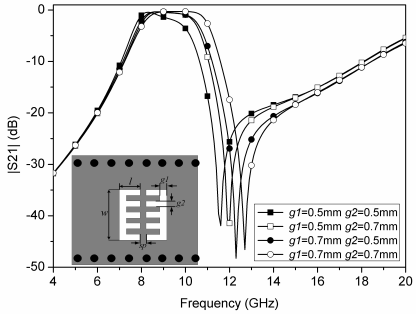

Figure 6. Simulated results of proposed DGS cell with variation of $g1$ and $g2$.

determined by the width of SIW as mentioned above. The different results caused by viable dimensions of DGS can be explained that the equivalent capacitance Cp is mainly determined by slot gaps while the equivalent inductance Lp is relative to the magnetic flux through the defect. As for the parameter of sp, it controls the inner coupling of the proposed DGS. To increase sp will decrease coupling so that the bandgap point of DGS moves to higher frequency. Therefore, an obvious advantage of the proposed DGS structure is that more parameters can be adjusted than conventional structures in order to achieve specific rejection band. What's more, according to the design requirement, cascading more DGSs can get a broader rejection bandwidth.

2.3. SIW T-junction Power Divider Loaded by DGS

The configuration of the proposed power divider based on SIW technology loaded by the proposed DGS is shown in Figure 7. It consists of a T-junction with an inductive post, three SIW to 50 Ω microstrip line transitions for testing convenience and three DGS cell which provides band stop function. The metallic vias fences form the narrow wall of the substrate integrated waveguide with the diameter of 0.4 mm. The space between two adjacent vias is 0.7 mm. The width of the SIWs is designed as 12.9 mm in order to make SIW to work at its dominant TE_{10} mode and to suppress the higher modes. The tapers from the SIWs to microstrip lines are with the same length of 3.2 mm, and width of 2.6 mm and 0.76 mm at the two ends, respectively. The width of the 50 Ω microstrip line is 0.76 mm. The inductive post placed at the centre of the power divider has great impact on the reflection and scattering of the input signals. After being optimized, the diameter and position of the inductive post are 0.8 mm and 0.1 mm.

The optimized values of all parameters are shown in Table 1.

Table 1. Geometrical sizes of the power divider (unit: mm).

symbol	value	symbol	value
S	0.7	W_{siw}	12.9
D	0.4	W_{taper}	1.6
l_post	0.1	l_{taper}	3.2
D_post	0.8	$w50$	0.76
y	9.6	l	2
w	5.1	gi	0.6

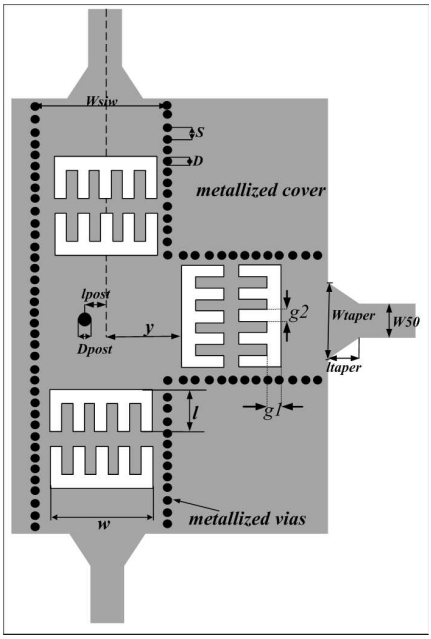

Figure 7. Model of the proposed power divider.

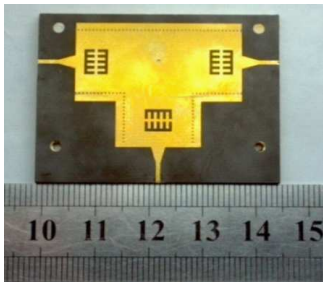

Figure 8. Photograph of the fabricated power divider.

3. EXPERIMENT AND MEASUREMENT RESULTS

As shown in Figure 8, the proposed band-pass power divider is fabricated using a single layer PCB process on RT/Duroid5880 substrate with relative permittivity of 2.2, loss tangent of 0.001 (at 10 GHz) and a thickness of 0.254 mm. The measurement is taken by using Agilent four-port vector network analyzer N5245A.

In Figure 9, the comparison between the measured and the simulated frequency responses is shown. It can be seen that there is a good agreement between the simulated results and the measured results. The measured insertion loss in the pass-band is better than 4.2 dB with imbalance of about 0.3 dB between the two output ports. And the measured input return loss is better than 17 dB across the bandwidth from 8 GHz to 9.4 GHz. Due to the SMA connector loss and the fabrication tolerance, the measured insertion loss is slightly larger than the simulated one. As for the isolation performance between port 2 and port 3, the isolation is only below 7 dB which is needed to be improved in our future work.

Figure 10 depicts the measured phase response of the proposed power divider, it can be seen that the proposed power divider gets a

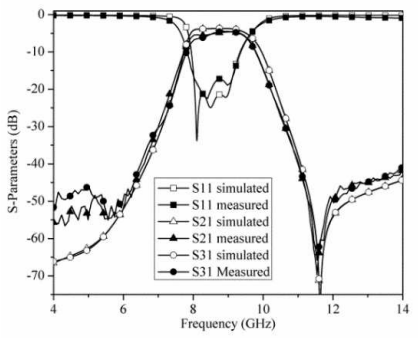

Figure 9. Comparison of measured and simulated frequency response of the proposed power divider.

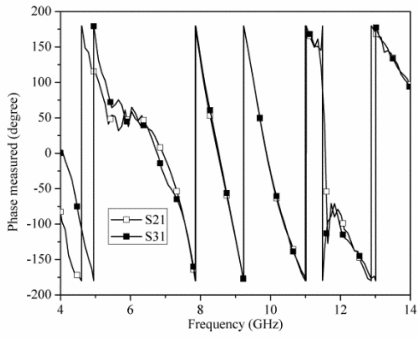

Figure 10. Measured phase response of the proposed power divider.

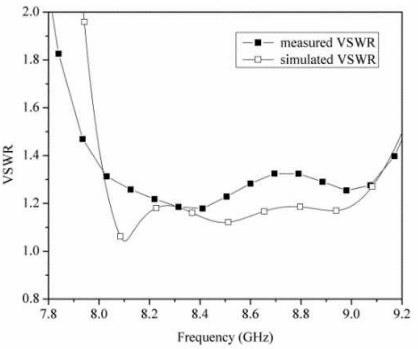

Figure 11. VSWR of the input port of the proposed power divider.

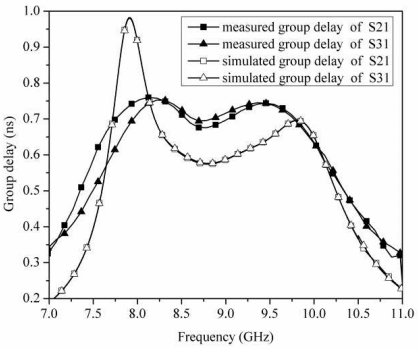

Figure 12. The simulated and measured group delay of the proposed power divider.

good phase performance within the pass band. Also there is a little imbalance of about 0.5 degree in the phase of the two output ports. One of the reasons is the discontinuity of the T-junction which leads to different wave distances for the two outputs. Another important reason is that the SMA connectors for testing are not entirely identical when the apparatus tests the multiport circuit. In addition, the fabrication tolerances cause the asymmetry of the geometry which can also lead to the phase imbalance.

Figure 11 illustrates the VSWR of the input of the proposed power divider, and it shows a good reflection performance.

Figure 12 shows the simulated and measured group delay at the two output ports of the band pass power divider. It can be seen that

the measured group delay in the pass-band is about 0.7 ns. And the group delay is quite smooth with variation of less than 0.1 ns which indicates that the proposed power divider gets a linear phase.

Table 2 illustrates the performance comparison between the proposed power divider and some reported power dividers integrated with filers [27–31]. It shows that this work has advantage of controllable bandwidth by easily adjusting the dimensions of SIW and DGS, and the insertion loss of the proposed power divider is relatively low as well as the amplitude and phase imbalance are very low too. In addition, the proposed band-pass power divider is relatively compact, it is smaller than other two SIW and HMSIW based band-pass power dividers in [29] and [30]. Although, the size of power divider in [27] and [31] is smaller than our proposed one, these two power dividers

Table 2. Comparison between this work and some other works.

Reference	Frequency (GHz)	Fractional Bandwidth (3-dB)	Insertion loss (dB)	Amplitude Imbalance (dB)
[27]	1.66–1.94 /2.69–3.11	8%/7.4%	< 0.8 / < 0.9	-
[28]	14.2–16.0	12%	< 1.4	< 0.5
[29]	12.2–12.8	4.8%	< 1	< 0.35
[30]	8.6–12.2	34.6%	< 1.6	< 0.6
[31]	1.373–1.629	8.6%	< 4.3	-
This work	8.0–9.4	16%	< 1.2	< 0.3

Reference	Phase Imbalance (degree)	Size (λ_g^{2*})	Topology	-
[27]	-	0.32/0.86	Microstrip line	-
[28]	-	-	HMSIW	-
[29]	2	8.64	Multilayer SIW	-
[30]	-	1.95	HMSIW	-
[31]	-	0.67	Wilkinson coupled-line	-
This work	< 0.5	1.90	SIW-DGS	-

$^*\lambda_g$ is the guided wavelength of the centre frequency of the passband.

are based on microstrip line which means they will suffer from high radiation loss when they are used in high frequency applications such as in microwave and millimeter wave circuits.

4. CONCLUSIONS

In this paper, a novel power divider based on SIW and DGS is proposed. It has advantages of controllable fractional bandwidth, high selectivity, and good in-band balance performance. Since the proposed power divider can get a band pass character, a filter can be erased when the proposed power divider is utilized in the system, so that it will lead to effective reduction of the size, loss and cost of the systems in the microwave and millimeter-wave applications.

ACKNOWLEDGMENT

This work was supported by Greating-UESTC Joint Experiment Engineering Centre, University of Electronic Science and Technology of China.

REFERENCES

1. Wilkinson, E., "An N-way hybrid power divider," *IEEE Trans. Microw. Theory Tech.*, Vol. 8, 116–118, Jan. 1960.
2. Deng, P.-H., J.-H. Guo, and W.-C. Kuo, "New Wilkinson power dividers based on compact stepped-impedance transmission lines and shunt open stubs," *Progress In Electromagnetics Research*, Vol. 123, 407–426, 2012.
3. Ruiz-Cruz, J. A., J. R. Montejo-Garai, J. M. Rebollar Machain, and S. Sobrino, "Compact full Ku-band triplexer with improved *E*-plane power divider," *Progress In Electromagnetics Research*, Vol. 86, 39–51, 2008.
4. Hosseini, F., M. Khalaj-Amir Hosseini, and M. Yazdani, "A miniaturized Wilkinson power divider using nonuniform transmission line," *Journal of Electromagnetic Waves and Applications*, Vol. 23, No. 7, 917–924, 2009.
5. Oraizi, H. and M. S. Esfahlan, "Miniaturization of Wilkinson power dividers by using defected ground structures," *Progress In Electromagnetics Research Letters*, Vol. 4, 113–120, 2008.
6. Shamsinejad, S., M. Soleimani, and N. Komjani, "Novel miniaturized Wilkinson power divider for 3G mobile receivers," *Progress In Electromagnetics Research Letters*, Vol. 3, 9–16, 2008.

7. Zhang, H., X.-W. Shi, F. Wei, and L. Xu, "Compact wideband Gysel power divider with arbitrary power division based on patch type structure," *Progress In Electromagnetics Research*, Vol. 119, 395–406, 2011.
8. Russo, I., L. Boccia, G. Amendola, and H. Schumacher, "Compact hybrid coaxial architecture for 3 GHz–10 GHz UWB quasi-optical power combiners," *Progress In Electromagnetics Research*, Vol. 122, 77–92, 2012.
9. Wu, Y. and Y. Liu, "An unequal coupled-line Wilkinson power divider for arbitrary terminated impedances," *Progress In Electromagnetics Research*, Vol. 117, 181–194, 2011.
10. Zhang, Z., Y.-C. Jiao, S. Tu, S.-M. Ning, and S.-F. Cao, "A miniaturized broadband 4 : 1 unequal Wilkinson power divider," *Journal of Electromagnetic Waves and Applications*, Vol. 24, No. 4, 505–511, 2010.
11. Wu, Y., Y. Liu, S. Li, and C. Yu, "Extremely unequal Wilkinson power divider with dual transmission lines," *Electronics Letters*, Vol. 46, No. 1, 90–91, 2010.
12. Kim, Y., "A 10 : 1 unequal Gysel power divider using a capacitive loaded transmission line," *Progress In Electromagnetics Research Letters*, Vol. 32, 1–10, 2012.
13. El-Tager, A. M. E., A. M. El-Akhdar, and H. M. El-Henawy, "Analysis of coupled microstrip lines for quad-band equal power dividers/combiners," *Progress In Electromagnetics Research B*, Vol. 41, 187–211, 2012.
14. Miao, C., B. Li, G. Yang, N. Yang, C. Hua, and W. Wu, "Design of unequal Wilkinson power divider for tri-band operation," *Progress In Electromagnetics Research Letters*, Vol. 28, 159–172, 2012.
15. Cassivi, Y., L. Perregrini, P. Arcioni, M. Bressan, K. Wu, and G. Conciauro, "Dispersion characteristics of substrate integrated rectangular waveguide," *IEEE Microw. Wireless Compon. Lett.*, Vol. 12, No. 9, 333–335, Sep. 2002.
16. Xu, F. and K. Wu, "Guided-wave and leakage characteristics of substrate integrated waveguide," *IEEE Trans. Microw. Theory Tech.*, Vol. 53, No. 1, 66–73, Jan. 2006.
17. Deslandes, D. and K. Wu, "Integrated microstrip and rectangular waveguide in planar form," *IEEE Microw. Wireless Compon. Lett.*, Vol. 11, 68–70, Feb. 2001.
18. Germain, S., D. Deslandes, and K. Wu, "Development of substrate integrated waveguide power dividers," *IEEE CCECE Canadian Conference on Electrical and Computer Engineering*, Vol. 3, 1921–1924, Canada, 2003.

19. Hirokawa, J., K. Sakurai, M. Ando, and N. Goto, "An analysis of a waveguide T-junction with an inductive post," *IEEE Trans. Microw. Theory Tech.*, Vol. 39, No. 3, 563–566, Mar. 1991.
20. Deslandes, D. and K. Wu, "Single-substrate integration technique of planar circuits and waveguide filters," *IEEE Trans. Microw. Theory Tech.*, Vol. 51, No. 2, 593–596, Feb. 2003.
21. Xu, F. and K. Wu, "Guided-wave and leakage characteristics of substrate integrated waveguide," *IEEE Trans. Microw. Theory Tech.*, Vol. 53, No. 1, 66–73, 2005.
22. Shao, Z. H. and M. Fujise, "Bandpass filter design based on LTCC and DGS," *Proc. Asia-Pacific Microwave Conf.*, Suzhou, China, 2005.
23. Weng, L. H., Y.-C. Guo, X.-W. Shi, and X.-Q. Chen, "An overview on defected ground structure," *Progress In Electromagnetics Research B*, Vol. 7, 173–189, 2008.
24. Ahn, D., J.-S. Park, C.-S. Kim, J. Kim, Y. Qian, and T. Itoh, "A design of the low-pass filter using the novel microstrip defected ground structure," *IEEE Trans. Microw. Theory Tech.*, Vol. 49, No. 1, 86–93, Jan. 2001.
25. Abdel-Rahman, A., A. R. Ali, S. Amari, and A. S. Omar, "Compact bandpass filters using defected ground structure (DGS) coupled resonators," *IEEE MTT-S International Microwave Symposium Digest*, 12–17, Jun. 2005.
26. Huang, Y., Z. Shao, and L. Liu, "A substrate integrated waveguide bandpass filter using novel defected ground structure shape," *Progress In Electromagnetics Research*, Vol. 135, 201–213, 2013.
27. Li, Y. C., Q. Xue, and X. Y. Zhang, "Single- and dual-band power dividers integrated with bandpass filters," *IEEE Trans. Microw. Theory Tech.*, Vol. 60, No. 1, 69–76, Dec. 2006.
28. Liu, B., "The application of image transition in HMSIW power splitter design," *High Speed Intelligent Communication Forum (HSIC)*, 1–2, May 2012.
29. Hui, J. N., W. J. Feng, and W. Q. Che, "Balun band pass filter based on multilayer substrate integrated waveguide power divider," *Electronics Letters*, Vol. 48, No. 10, 571–573, 2012.
30. Zou, X., C.-M. Tong, and D.-W. Yu, "Y-junction power divider based on substrate integrated waveguide," *Electronics Letters*, Vol. 47, No. 25, 1375–1376, 2011.
31. Deng, P.-H. and L.-C. Dai, "Unequal Wilkinson power dividers with favorable selectivity and high-isolation using coupled-line filter trans-formers," *IEEE Trans. Microw. Theory Tech.*, Vol. 60, No. 6, 1520–1529, Jun. 2012.